Available online at www.sciencedirect.com
SCIENCE DIRECT®
Biochimica et Biophysica Acta 1661 (2004) 26–39
BIOCHIMICA ET BIOPHYSICA ACTA
BBA
www.bba-direct.com

Molecular dynamics study of the KcsA channel at 2.0-Å resolution: stability and concerted motions within the pore

Mylène Compoint[a], Paolo Carloni[b], Christophe Ramseyer[a,*], Claude Girardet[a]

[a] *Laboratoire de Physique Moléculaire, UMR CNRS 6624, Faculté des Sciences, la Bouloie, Université de Franche, Comté, 25030, Besançon Cedex, France*
[b] *International School for Advanced Studies (SISSA), Via Beirut 4, 34014, Trieste, Italy*

Received 21 July 2003; received in revised form 20 November 2003; accepted 24 November 2003

Abstract

The stability of the KcsA channel accommodating more than one ion in the pore has been studied with molecular dynamics. We have used the very last X-ray structure of the KcsA channel at 2.0-Å resolution determined by Zhou et al. [Nature 414 (2001) 43]. In this channel, six of the seven experimentally evidenced sites have been considered. We show that the protein remains very stable in the presence of four K^+ ions (three in the selectivity filter and one in the cavity). The locations and the respective distances of the different K^+ ions and water molecules (W), calculated within our KWKWKK sequence, also fits well with the experimental observations. The analysis of the K^+ ions and water molecules displacements shows concerted file motions on the simulated time scale (≈ 1 ns), which could act as precursor to the diffusion of K^+ ions inside the channel. A simple one-dimensional dynamical model is used to interpret the concerted motions of the ions and water molecules in the pore leading ultimately to ion transfer.

1. Introduction and historical survey of KcsA channels

Although the presence of the membrane helps cells to retain vital ingredients, ion permeation is crucial for a variety of biological functions such as nervous signal transmission and osmotic regulation. Ion channels are proteins inserted in the membrane lipid bilayer that form aqueous pores. They allow ions to cross the hydrophobic barrier of the core membrane, guaranteeing to the cell a controlled exchange of ionized particles. As all membrane proteins, ionic channels are difficult to crystallize and up to 1995, no high-resolution structure of a potassium channel was available. In 1995, the cloning of the first bacterial gene from *Streptomyces lividans* encoding for a potassium selective channel (the KcsA gene) [1] opened the avenue to a large production of purified K^+ channels and led in 1998 to the KcsA channel crystallization [2]. To date, several 3D KcsA structures available in the Protein Data Bank (PDB) have been determined by X-ray measurements or electron paramagnetic resonance (EPR) experiments. The X-ray structures were obtained at different resolutions using various ionic species (K^+,Rb^+ and tetrabutylammonium TBA) and concentrations [2–4]. The original X-ray structure (PDB code 1BL8) at 3.2-Å resolution was solved in the presence of 150 mM K^+ ions at pH 7.5 [2]. More recently, a structure has been solved at higher resolution (2.0 Å, PDB code 1K4C) at high K^+ concentration [4].

The crystallization of the KcsA and the determination of its structure by X-ray diffraction has allowed an unprecedented investigation of diffusion channels using theoretical calculations based on microscopic description of the interactions inside the protein. In particular, the permeation [5–9], the selectivity between ions [10–15], the diffusion [11,12,16] and more recently the gating [17–19] of KcsA channel have been investigated within the 3.2-Å description.

Very recently, Chung and Kuyucak [20] underlined the progress and prospects that the structure determined at 2.0-Å resolution could lead. To our knowledge, no calculation has been performed on this refined structure. In this paper, we focus on the first main result addressed by Zhou et al. [4] concerning the occurrence of new ion binding sites. Indeed, the determination of the 3.2-Å resolution structure [2] together with numerous molecular dynamics simulations

* Corresponding author. Tel.: +33-381-66-64-75; fax: +33-381-66-64-82.
E-mail addresses: mylene.compoint@univ-fcomte.fr (M. Compoint), christophe.ramseyer@univ-fcomte.fr (C. Ramseyer).

0005-2736/$ - see front matter © 2003 Elsevier B.V. All rights reserved.
doi:10.1016/j.bbamem.2003.11.019

[6,9–12,15,16,21–24] based on this structure suggested that the pore could accommodate several ions. The structure at higher resolution reveals additional sites which have not yet been fully studied on a numerical point of view. The aim of this paper is to confirm the experimental observation obtained on the 2.0-Å resolution structure using a classical microscopic molecular dynamics approach. We have studied the stability of this structure in the presence of ions located inside the proposed ion sites. In addition, we have analyzed the concerted motions of the ions inside the selectivity filter. Our approach follows the work previously done by Guidoni et al. [10,21] on the 3.2-Å resolution structure. This allows us a direct comparison with their results and the experimental findings.

In Section 2, we give a brief information on the different parts of the KcsA channel and compare the experimental structures at the two resolutions. Section 3 deals with the construction of the channel pore encapsulated inside its hydrophobic membrane and the molecular simulation set-up. In Section 4, we show the results of the dynamics of the K^+ ions, water molecules and pore walls for the 2.0-Å resolution structure and compare them to the preexisting theoretical results obtained on the 3.2-Å structure. We finally discuss in Section 5 the dynamics of the elements constituting the channel in terms of a simple mechanical model in order to propose a concerted diffusion mechanism inside the channel.

2. Comparison between the 3.2- and 2.0-Å experimental structures

2.1. General features of the KcsA channel

All the KcsA structures referenced in the PDB bank exhibit similar trends which are common to a large number of potassium channels. Several structural zones can be distinguished in this pore, namely a selectivity filter, a central cavity and a gate [2], which are responsible for the specific properties of the channel (selectivity, permeation and gating). A classical figure of the pore representing two subunits of KcsA channel with the extracellular side on top is displayed in Fig. 1. Each subunit contains two transmembrane helices (M_1 and M_2) between which there is a reentrant P-loop made by a descending P-helix (P) and an ascending filter (F) region containing the TVGYG sequence motif, common to all potassium channels and ensuring the selectivity to K^+ ions. From this, it can be seen that there are constrictions at both the extracellular and intracellular ends of the channel, with a wider central cavity C. The extracellular constriction corresponds to the selectivity filter F. The intracellular constriction, formed by the inner helix bundle, corresponds to the gate G.

In fact, potassium and other ion channels are proteins that switch between closed and opened conformations in response to an external stimulus in a process known as gating.

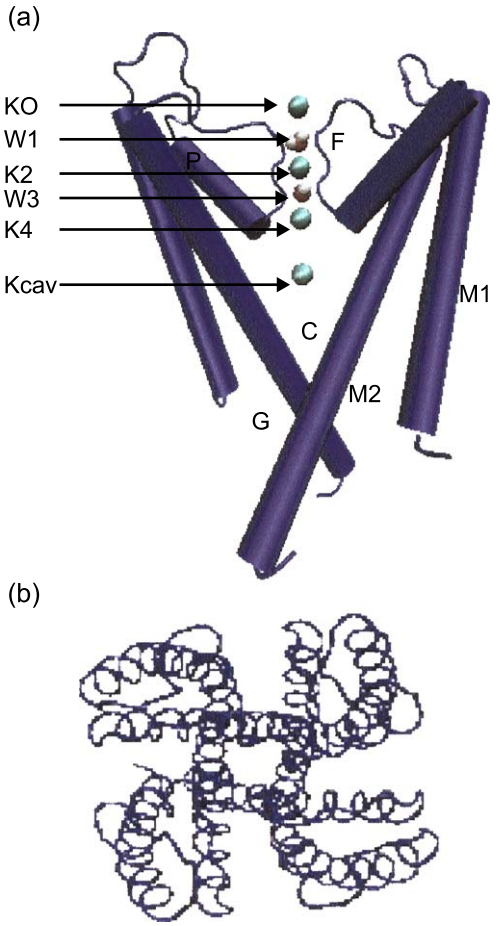

Fig. 1. Cylinder representation of the KcsA channel. For clarity, only two of the four subunits that make up the channel are shown. The initial KWKWK. . .K sequence of K^+ and water molecules is shown with K^+ ions in green spheres and water molecules in red and white. The initial locations within the channel are labelled K_0, K_2, K_4 and K_{cav} for K^+ ions and W_1 and W_3 for water molecules. The selectivity filter (F), the cavity (C), the gate (G), the M_1 and M_2 helices, and the P-helices are also labelled.

Two general categories of ion channel gating are defined by the initiating stimulus: ligand binding (neurotransmitter or second-messenger-gated channels) or membrane voltage (voltage-gated channels like KcsA). The mechanism of the gating is actually not well understood and remains a challenge for the scientific community which works in this field of interest [25,26]. It is quite sure that large conformational changes occur in the gate zone [27,28]. Nevertheless, questions remain about how and why the inner helices move to open the pore and how wide the pore becomes. In the KcsA structure, the pore is very wide (about 12-Å diameter) at the center of the central cavity, but close to the gate G, the diameter narrows to about 4 Å. Note that the filter region F is also narrow with a radius of 1.4 Å and a length of 12 Å, and it contains ion-binding sites formed by rings of backbone oxygen atoms oriented toward the pore axis. The water-filled cavity provides an energetically favorable environment for a K^+ ion in the hydrophobic interior of a membrane.

2.2. Differences between the 3.2- and 2.0-Å experimental structures

The comparison of the protein structure of KcsA determined at resolutions of 3.2 Å [2] and 2.0 Å [4] does not show fundamentally different structural changes. The residues forming the selectivity filter and the cavity remain nearly the same. Nevertheless, the most refined structure reveals six extra amino acids per subunit which are located at the end of the helix bundle and at the water/membrane interface in the intracellular side (see Fig. 2). These residues should certainly play an important role in the gating knowledge [28] but their role is not still elucidated. Another difference concerns the occupancy of the pore by K^+ ions and water molecules. In the previous experimental observations and numerical simulations based on a microscopic description of the channel, it was shown that the pore could accommodate several ions at one time. In the 3.2-Å resolution X-ray structure, three ion binding sites, S_1, S_3 and S_4 (upper site, upper inner site and tower inner site) (Fig. 3), were identified within the filter, while seven were found in the 2.0-Å resolution structure. Indeed, in addition to the four positions S_1–S_4 determined inside the filter, one was found in the cavity (S_{cav} in Fig. 3), one in the extracellular side of the membrane (S_{EXT}, not shown) and the last one at the outer mouth of the channel (S_0 in Fig. 3). Note that these additional sites were yet predicted by Berneche and Roux [16] on the basis of free energy surface calculations applied to the 3.2-Å resolution structure. In their paper, the authors showed that, even though no large free energy barrier opposing ion conduction is observed, five specific sites are revealed in the selectivity filter by the superimposition of a few number of two-dimensional free energy maps. The 2.0-Å resolution crystal structure revealed further details on both hydration and coordination of ions within the filter. These studies suggested that total or partial dehydration of the K^+ ions should occur for the permeation. Indeed, the coordination of the 4 K^+ ions within the filter at each of the four sites (S_1 to S_4) is made up of eight oxygen atoms belonging to the protein. The sites located in the cavity and in the outer mouth conserve their natural hydration shell while S_0 is formed by four oxygen atoms from the carbonyl of Gly79, with the remaining interactions provided by water molecules. Thus, the K^+ ion's hydration shell has been half-replaced by interactions with oxygen atoms of the protein.

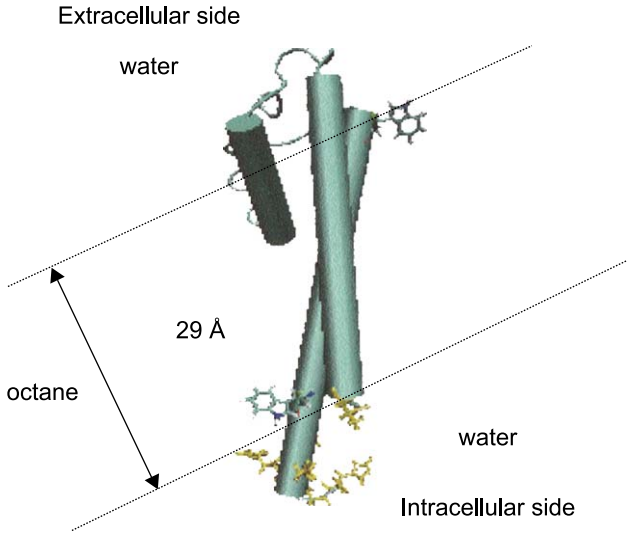

Fig. 2. Immersion of the KcsA structure in a water/octane/water bilayer. The octane slab is comprised between the dashed lines. One protein monomer is represented with residues limitating the octane slab in blue (Trp87 and Trp113). Additional residues which appear in the 2.0-Å resolution structure and not in the 3.2-Å resolution structure are shown in yellow.

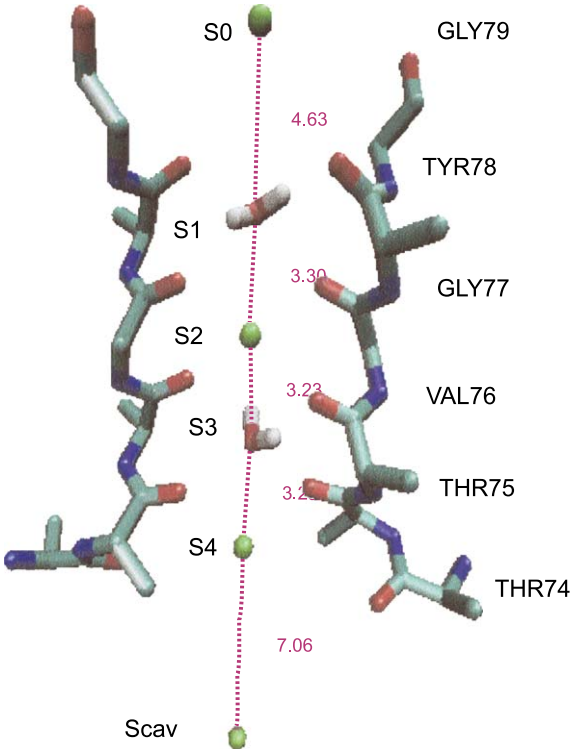

Fig. 3. Model used for the MD simulation with crystallographic sites (see Ref. [4]) occupied by ions and water molecules along the channel axis. Distances are also reported. Note that the seventh site at the extracellular side S_{ext} is not shown here.

3. Model system for the KcsA channel and simulation set-up

3.1. Description of the system

The closed potassium channel was built using the KcsA structure (PDB code 1K4C) established at high resolution (2.0) [4]. On the basis of the experimental observations, the model structure contains 534 amino acids, 7 K^+ ions, 469 water molecules and 2 partial lipids. The additional 24 amino acids occurring in the 2.0-Å resolution structure are located at the end of the protein in the intracellular side of

the membrane. They correspond to Ser22, Glu120, Arg121, Arg122, Gly123, His124 in one subunit. Part of the side chains of six amino acids (Leu24, Arg27, Tyr62, Leu86, Arg117 and Arg121) missing in the X-ray structure was also added using standard residue geometries and taking care to avoid unphysical contacts. The His25 located in the intracellular side of the membrane was assumed to be protonated in the N_δ position since His25 can form an H-bond with carbonyl group of Ala109 and an oxygen of Tyr133. We have chosen to protonate Glu71 side chain because it is involved in a strong hydrogen bond with Asp80. The missing amino acids are those located in the ligand receptors located at the membrane surface on the extracellular side. This part of the protein is not considered in the present study.

We have also taken into account the protein surrounding [10,21]. The lipid bilayer of the cellular membrane (hydrophobic area) is modelled by an octane box, which was shown to be efficient to mimic the lipid behavior [10,21,23] (see Fig. 2). In a box of about 73 $Å^3$, we have immersed the portion of protein ranging from Trp87 and Trp113 inside an octane slab of 29 Å of thickness (see Fig. 2). The remaining part of the protein is hydrated with water molecules. On both sides of the octane slab, the extracellular and intracellular sides are formed also by a slab of 22-Å thickness of water molecules. It should be noted that we have also used information given by the experimental KcsA structure to better model the different aqueous areas. For instance, we have kept 226 crystallographic water molecules lying at less than 4 Å from the protein either on the internal or external sides of the membrane. We have also kept the 16 water molecules determined in the cavity. Note that we have filled the cavity with 38 water molecules, namely we have added 22 molecules more in order to be consistent with previous calculations [10,21,22]. It should be mentioned that we must distinguish the behavior of the water molecules which constitute the solvent (intra- and extracellular areas) from those which hydrate the cavity. Therefore, the density of bulk water has been chosen for molecules in the extra- and intracellular sides while the density of water molecules in the cavity was determined by evaluating the Connolly surface [29].

The pore axis contains K^+ ions and water molecules. Among the seven ionic sites elucidated in the 2.0-Å resolution structure [4] (two extracellular sites S_0 and S_{EXT} and five sites inside the channel S_1 to S_{cav}), we only deal with sites S_0 to S_{cav} because S_{EXT} appears at high K^+ concentration only. Inside the filter, the filling distribution by K^+ ions and water molecules is not random. It has been suggested that two K^+ ions should be separated by a water molecule [16,22,30] in order to increase the solvation of K^+ ions. Although this quasi-linear KWK sequence remains intuitive, its existence could be understood when considering steric effect (the K^+ radius and the average radius of a water molecule are, respectively equal to 1.33 and 1.41 Å) and the strong repulsive interaction occurring if one considers that two K^+ ions lie in nearest neighbor positions. Our chosen sequence is thus KWKWK. . .K which corresponds to two water molecules in the S_1 and S_3 sites and four potassium ions (three inside the channel and one in the cavity otherwise filled by water molecules) at the S_0, S_2, S_4 and S_{cav} crystallographic sites, respectively. Fig. 1 shows this starting configuration in a schematic representation of the protein. Fig. 3 details this sequence within the selectivity filter and gives the distance between ions or water molecules issued from the experiments [4]. The distance between the two ions located in S_4 and S_{cav} sites is rather large (about 7 Å). This allows the two ions to stay in neighboring positions, especially if the ion in the cavity is fully hydrated. This feature has been verified by Guidoni et al. [10,21] in molecular dynamics studies using the 3.2-Å resolution structure. They showed that the K^+ ion retrieves its complete solvation shell (eight water molecules) in the cavity filled by at least 30 water molecules. Let us remind that in our model, the cavity contains 38 water molecules. This number is sufficient to fully hydrate the ion. Finally, there remains 28 positively charged Arg residues and 16 negatively charged residues (12 Glu and 4 Asp). The remaining positive charge of the protein (+12) was neutralized by ions (20 Cl^-, 4 Na^+ and 4 K^+). The electro-neutral system thus contains 35 827 atoms.

3.2. Simulation backgrounds

This initial, average, geometry of the system given by experiments [4] did not appear to be stable. To proceed, we have thus established the following equilibration protocol. We have first minimized the energy of the total system formed by the octane slab and the two water slabs during 72 ps at 0 K, half time by constraining the protein backbone and the other half time by releasing the protein structure. Then, the solvent (octane and water) was free to move for 110 ps of MD at constant volume by increasing smoothly T up to 300 K and keeping the protein backbone fixed at its minimized structure at 0 K. In the third step (330 ps), the protein was relaxed in (N,V,T) conditions very smoothly during 45 ps (15 ps by keeping the K^+ ions and the backbone constrained, 15 ps with the K^+ ions and filter constrained and 15 ps with K^+ ions constrained). The temperature was also smoothly increased by following the same protocol used for the membrane equilibration. Finally, we switched to the (NPT) conditions during 1.1 ns at 300 K. Note that the resulting time required to equilibrate the system was about 1.61 ns. For the results, we focus on the protein dynamics and only 1.43 ns is reported. This time was also shown to be sufficient to reach equilibrium for the protein built on the basis of the 3.2-Å resolution structure [10,21].

The simulations were performed with the AMBER suite of program using the AMBER6 force field. The coulomb interactions were treated using the particle mesh Ewald method [31]. Water molecules were described by the TIP3P

model [32]. Time step of 1 fs was required to describe all external movements, including the water rotations. Simulations were performed in the (NVT) or (NPT) ensembles using the approach proposed by Bernèche and Roux [22]. The NVT conditions were first applied to stabilize the protein [10,21] and then we switch to NPT conditions in order to allow relaxation of the system during the dynamics. Here, we want to focus on this change of dynamics conditions since this event can be viewed as a constraint release from NVT to NPT ensembles inducing a perturbation on the system. In the following discussion, we will see that this peculiar event can be assimilated to mechanical fluctuations of the protein possibly responsible for the diffusion in the pore. The temperature was maintained to a constant value using the Berendsen's thermal coupling [33] at 1-fs relaxation time.

The dynamical information given in the simulation is analyzed through the mean square displacements of the atoms, ions and molecules and the time correlation functions of these displacements. The mean square displacement σ is conventionally written as

$$\sigma_r(t) = \left[\frac{1}{N}\sum_{i=0}^{N}(\mathbf{r_i}(\mathbf{t}) - \mathbf{r_i}(\mathbf{0}))^2\right]^{1/2} \quad (1)$$

where $\mathbf{r_i}$ defines the position (x_i,y_i,z_i) of the ith atom at time t or at the beginning of the production phase. N is the total number of atoms and T_s is the duration of the simulation. Note that we will also consider mean square displacements σ_z along the pore axis of the atoms, ions and molecules.

In a similar way, the time correlation function for the displacements of two atoms, ions or molecules named i and j is written as

$$C_r^{ij}(\tau) = \frac{1}{T_s/2}\int_0^{T_s/2}\frac{\sum_i \mathbf{\Delta r_i}(\mathbf{t}+\tau)\mathbf{\Delta r_j}(\mathbf{t})}{\sum_i \mathbf{\Delta r_i}(\mathbf{t})\mathbf{\Delta r_j}(\mathbf{t})}\mathrm{d}t \quad (2)$$

where $\mathbf{\Delta r_i}$ defines the displacement of the ith atom relative to its origin. $C_z^{ij}(\tau)$ will thus correspond to the correlation function along the pore axis and $C_r^{ii}(\tau)$ to the autocorrelation function.

4. Results

4.1. Stability of the protein and ions within the KWKWK...K sequence

We have reported the root mean square displacements (rmsd) σ_r of some characteristic parts of the KcsA channel. During the 1.43 ns of the production phase in the simulation, the protein remains very stable since the rmsd experienced by the C_α, C, N and O atoms for all residues of the protein does not exceed 0.4 Å in average when the volume is constrained (Fig. 4). Switching at 360 ps from NVT to NPT conditions leads to a continuous drift of the rmsd during about 400 ps. Then the rmsd value remains nearly constant and stabilizes around 1.3 Å. The protein has reached a new equilibrium. The region corresponding to the selectivity filter remains also

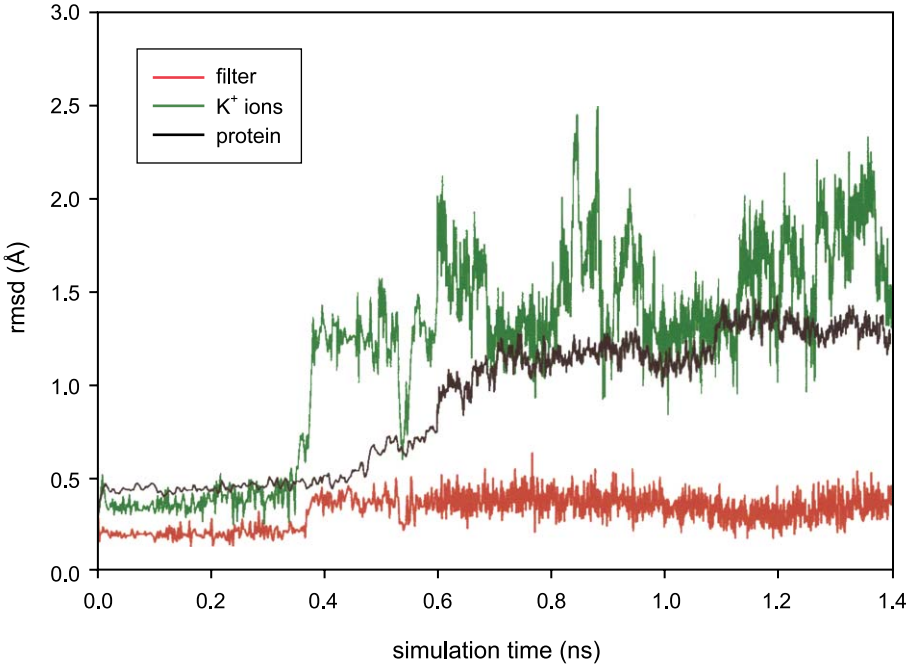

Fig. 4. Root mean square displacements σ_r of the protein backbone (black), the filter (red) and the K^+ ions (green) inside the KWKWK...K file along the overall production phase of the dynamics (1.4 ns).

very stable (rmsd less than 0.5 Å) while the ions located into the file experience larger fluctuations (2 Å at maximum). We can see that the filter and the ions move abruptly (less than 10 ps) during the change from NVT to NPT when compared to the protein motions. This is simply because the protein contains 6284 atoms and the change of dynamical ensemble produces progressive effects on all atoms. We have also calculated the rmsd's for separated parts of the selectivity filter (figures not shown here). Very small values are obtained (about 0.1–0.2 Å) indicating that no significant deformation of the filter occurs. Nevertheless, residues located at the extremities of the filter (Thr74 and Gly79) have much more pronounced motions since they are partially in contact with water molecules in the cavity for Thr74 and at the extracellular interface for Gly79. This corroborates the feature that the structure of KcsA crystal in the presence of a low concentration (3 mM) of K^+ ions exhibits a certain degree of flexibility [4,9] though it remains very rigid.

In Fig. 5, we have reported, in addition to the starting configuration chosen as the crystallographic sites (a), the average positions obtained from the simulation of each ion in the pore (b) and a typical snapshot showing large deviations from the average positions(c). The distances listed on the average structure (Fig. 5b) fit nicely with the distances resolved experimentally (Fig. 5a). The average distance between K_4 and K_{cav} is nearly the same since it is equal to 7.29 Å in our calculations while it has been determined to be 7.06 Å experimentally. The comparison is also satisfactory for the calculated distances between water molecules and K^+ ions inside the filter. The main discrepancy occurs for the position of the K_0 ion at the outer mouth of the selectivity filter. Our calculated distance 2.6 Å is much smaller than the value of 4.63 Å found by X-ray measurements. The fact that this site is closer to the pore has already been observed in simulations by Bernèche and Roux [16]. In addition, they found that K_0 leaves its position toward the extracellular side only when the ion in the cavity pushes the two ions in the selectivity filter. This indicates also the strong stability of the K_0 site. A possible explanation of such a difference in the distance could originate in the fact that the finite concentration of K^+ ions inside the intra- and extracellular sides of the channel is far to be the experimental one. We will see, however, that the unexpected localization of K_0 ion will not change its further behavior regarding its diffusion toward the extracellular side. Another explanation could be due to the fact that the experimental structure was obtained on a crystallized structure at low temperature. Thus, one could think that the positions we obtain here, at 300 K, are different especially at the outer mouth of the filter. The discrepancy with the X-ray experiments might also have been caused by other factors like buffers, addition of anti freeze such as PEG, bound antibody, etc.

As a conclusion, these results support the suggestion that KcsA (and by extension other K channels) is a multi-ion pore and it can accommodate a succession of up to six sites in a row in capable of binding four K^+ in a very stable manner.

4.2. Correlated motions within the KWKWK...K file

In Fig. 6 the displacements σ_z along the pore axis z of the six sites in the filter are drawn vs. time, including the switching from NVT to NPT ensemble. They show three

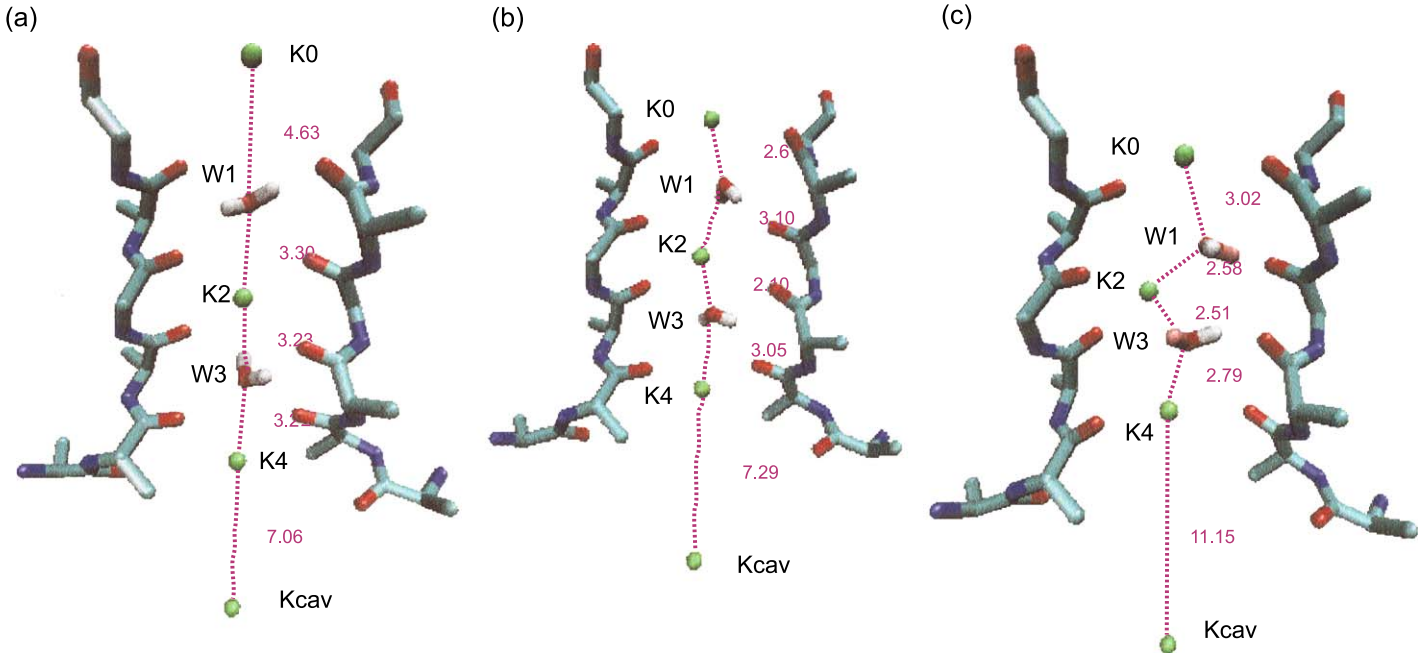

Fig. 5. Locations of potassium ions (green) and water molecules (red and white) along the channel axis during the MD simulation. The distances between ions and water molecules are also reported. Location and labelling of the ions at the beginning of the MD (a), in average during the MD (b) and in an extreme situation when K_4 undergoes large motions (c).

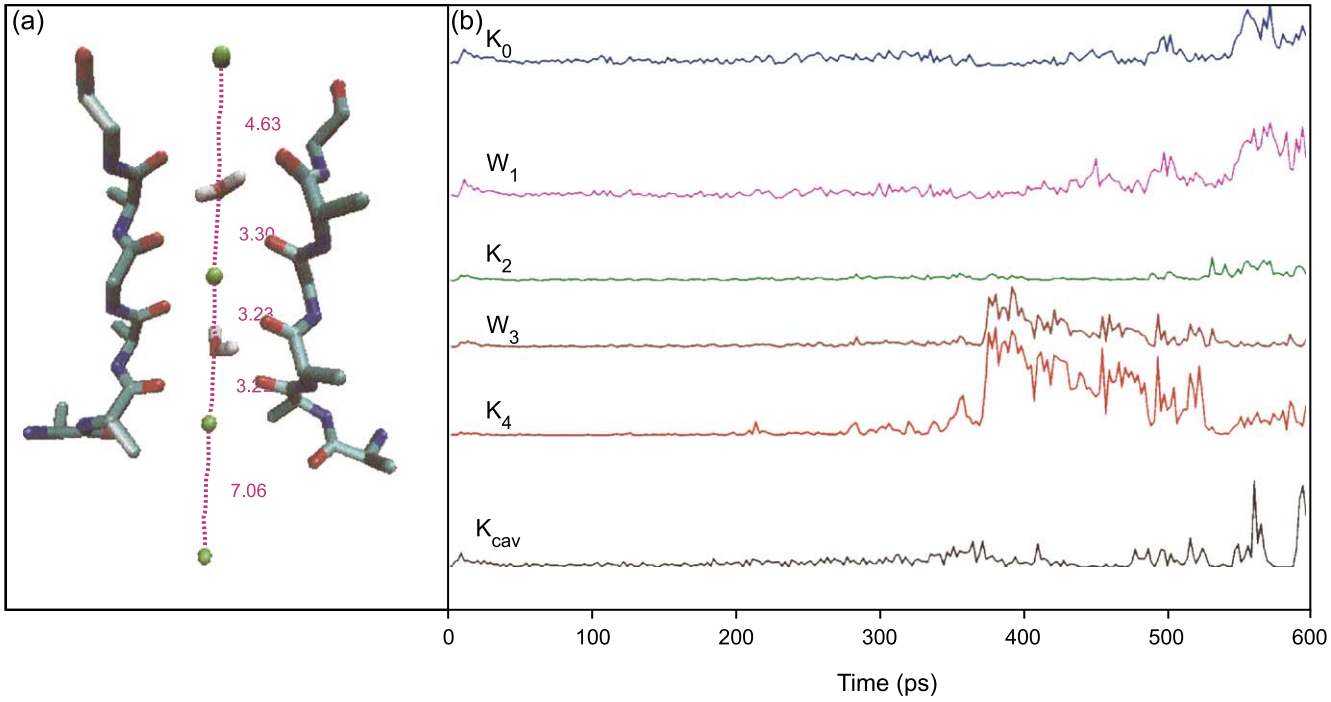

Fig. 6. Schematic representation of the KWKWK. . .K file location inside the pore (a) and corresponding z square displacement of K^+ ions and water molecules along the pore axis for the first 600 ps of the production phase.

main features which are at the origin of concerted motions within the KWKWK. . .K file. First, the K_2 site remains stable during all the time of the simulation, even if it feels the change of MD ensemble 200 ps later. Such a stability is consistent with previous data, since this site has been for a long time clearly elucidated both by X-ray experiments and MD simulations [10]. It is strongly stabilized by the electrostatic interactions between the ion and the eight carbonyl groups coming from Val76 and Gly77 in its neighboring. A simple point electrostatic calculation corroborates this argument. The potential energy experienced by a positive charge displaced along the pore axis would show a very stable site located precisely at the K_2 position.

Second, the other K^+ ions have generally much larger magnitude motions. A closer examination of the rmsd's along z axis of each K^+ ion shows that K_{cav} remains in average in the cavity site with large motions around it. More surprising are the displacements of K_4. This ion is a priori the less stable site of the KWKWK. . .K file, especially when the system is perturbed by the switch to NPT conditions. It succeeds in stabilizing 200 ps after this switch but undergoes much larger motions than the other K^+ ions during this delay. In Fig. 5c, it is clear that K_4 can leave its average site to approach another position where it bounds preferentially to the oxygen atoms of Thr75 carbonyl groups. It seems therefore that K_4 can explore two non-equivalent wells. In the most favorable site, the K^+ ion interacts directly with the oxygen atoms located on the carbonyl groups of Thr75 and those of the hydroxyl groups of Thr74 (Fig. 5b). In the second site just above the Thr75 carbonyl groups (Fig. 5c), the electrostatic interactions with this residue are clearly more favorable than those with Thr74 residue. Nevertheless, on the first site close to the starting configuration, K_4 is more hydrated when it faces the Thr74 residues than when it faces Thr75. This subtle competition between hydration and electrostatics leads finally to the peculiar behavior where K_4 undergoes relatively large movements to explore these two configurations.

Third, and that is probably a major indication given by Fig. 6, the motions of the water molecules W_1 and W_3 close to K_0 and K_4 ions, respectively, are not random. Indeed, K_0 and W_1 move in a concerted manner like the other couple W_3 and K_4. In addition, the couple (K_4–W_3) seems to be rapidly excited by the switching (NVT/NPT) while all the other particules K_0, W_1, K_2 and K_{cav} start their motions later.

Fig. 7 lightens these interesting behaviors. It exhibits the square displacements σ_z of the two couples (K_0–W_1 and K_4–W_3) along the pore axis with respect to their average positions. The behavior of the two curves for each couple is nearly the same. For instance, K_0 and W_1 move exactly at the same time with the same amplitude, leading to perfect concerted motions. The slopes of the curves are also remarkably the same. They characterize the drift velocities of the species which are equal in average to 0.007 ± 0.001 Å ps^{-1} in each case. K_4 and W_3 show also concerted motions (same time and slopes) with however larger motions for K_4 when compared to W_3. This difference in amplitude has already been mentioned and it should correspond to a dynamical damping with coupled motions between protein atoms and ions. We remark that K_0 moves less than W_1 whereas K_4 moves more than W_3. This could confirm the presence of a

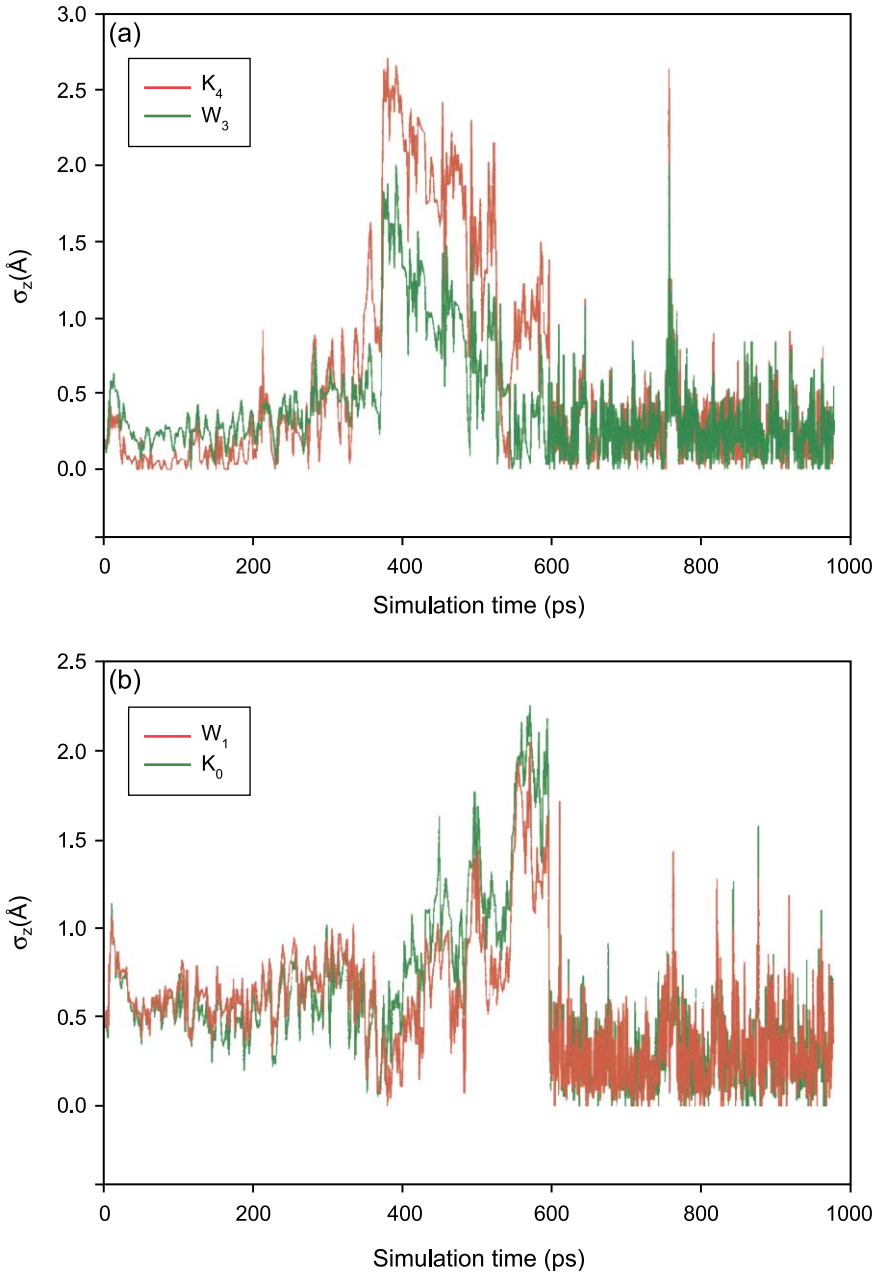

Fig. 7. Square displacements σ_z of (a) W_3-K_4 and (b) K_0-W_1 couples along the pore axis showing the correlations within the KWKWK...K file.

second site for K_4 ion, and explain the larger motions of this ion against W_3. In addition, there is also a concerted motion between the two couples K_4-W_3 and K_0-W_1 but shifted in time: the couple K_4-W_3 moves first and, when it is stabilized, the second couple K_0-W_1 starts to move. The role of K_2 on the adjacent water molecules is quite singular since W_1 and W_3 undergo similar motions with the external K_0 and K_4 ions but not with the internal K_2 ion.

All these features are reinforced by the behavior of the correlation functions $C_z^{ij}(\tau)$ between two ions, or between one ion and a water molecule along the axis coordinate z represented in Fig. 8. For the correlation times studied here, the K_0-W_1, K_4-W_3 and K_4-K_{cav} couples are strongly correlated up to 300 ps since the correlations are greater than 0.5 whatever the ensemble considered (NVT or NPT). To show the correlation between the two couples K_0-W_1 and K_4-W_3, we have calculated the correlation function for the pair K_0-K_4 which appears still to be significant in the same time interval. In Fig. 8, we see that the motion of K_2 in the filter and K_{cav} in the cavity are also strongly correlated, a feature that can already be observed in Fig. 6 although the motions of the ion in the cavity have a much larger magnitude.

Note in Fig. 7 that after 700 ps the couples (K_0-W_1) and (K_4-W_3) do not shift significantly in average from their stable configuration, excepted at some more or less regular times where the motions can reach 1.5 Å for the first couple

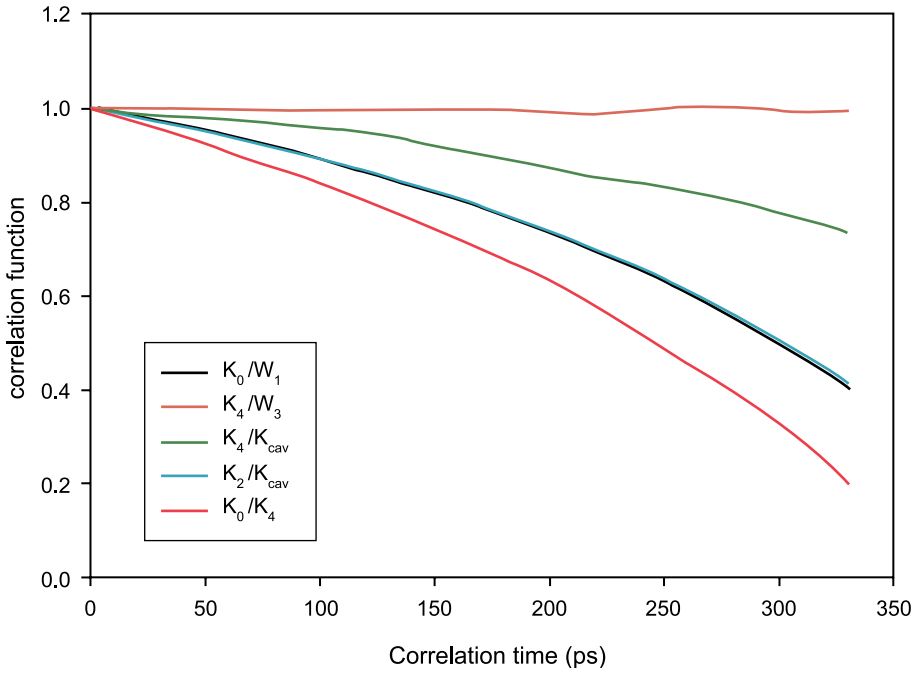

Fig. 8. Time correlation functions along the z direction for different couples of atom and water molecules couples showing the correlations within the KWKWK. . .K file.

and 2.5 Å for the second couple. The event at 750 ps observed for the couple (K_4–W_3) is particularly striking since the magnitude of the rmsd is similar to the displacement observed when the NVT conditions are switched to NPT ones, although there is no a priori deformation of the protein structure. This large motion over very short times (less than a few tens picoseconds) can be interpreted as resulting from a back and forth jump of K_4 in its two adjacent wells discussed before, and seems to corroborate the idea developed by Berneche and Roux concerning the knock-on diffusion mechanism [16,34]. Other similar typical events in the rmsd of (K_4–W_3) couple not shown here have also been observed at larger simulation times, indicating preliminary processes toward the diffusion of K^+ in the filter. Although less pronounced, events of this kind are also seen for the other couple (K_0–W_1), in strong correlation with the other couple motions.

4.3. Correlated motions between the ions and the filter atoms

We have already mentioned that the motions of the K^+ and W species contained in the filter are dynamically coupled to the atoms located at the internal part of the filter in the protein amino acids. As an example, we have analyzed these couplings for K_0 and W_1 located near the extracellular mouth with one of neighboring amino acids Tyr78. Fig. 9a exhibits the root mean square displacements σ_z of K_0 and W_1 together with those of the oxygen atoms belonging to the carbonyl groups of Tyr78. These species clearly move simultaneously with nearly the same amplitudes. This type of correlated motions with strong couplings indicates that the filter is not fundamentally distorted in that zone since the species move in a concerted manner. We have also done this investigation for the less mobile ion, namely K_2, and its neighboring amino acids Val76 and Gly77 located deeper in the selectivity filter. The situation illustrated in Fig. 9b is rather different from what happens in the extracellular part of the filter. Indeed, small K_2 fluctuations induce large motions of its neighbors Val76 and Gly77. The distortions induced by K_2 confirm the strong stability of this site and indicate that K_2 motions are significantly damped by the protein.

4.4. Hydration of ions

The average positions of the ions inside the filter and the cavity can be interpreted in terms of hydration. Fig. 10 displays the initial and average oxygen density as viewed by each K^+ ion. The case of K_4 is interesting since we have shown that even if its average location is well known, this ion experiences large amplitude motions in order to explore two sites, a stable and a metastable one. Fig. 10 shows that K_4 is surrounded in average by five to six oxygen atoms in its more stable site. When it is located in its metastable site, it fills also six oxygen neighbors. Between these two configurations K_4 needs to partially dehydrate. This loss of energy is partially compensated by the gain in electrostatic interactions with the Thr75 residue. Fig. 10 also reinforces the conclusion concerning the very large stability of K_2 since its number of coordination reaches up to 10 oxygen atoms at 3.2 Å: eight atoms come from the protein (Val76 and Gly77 residues) while the two others are the oxygens of the W_1 and W_3 molecules.

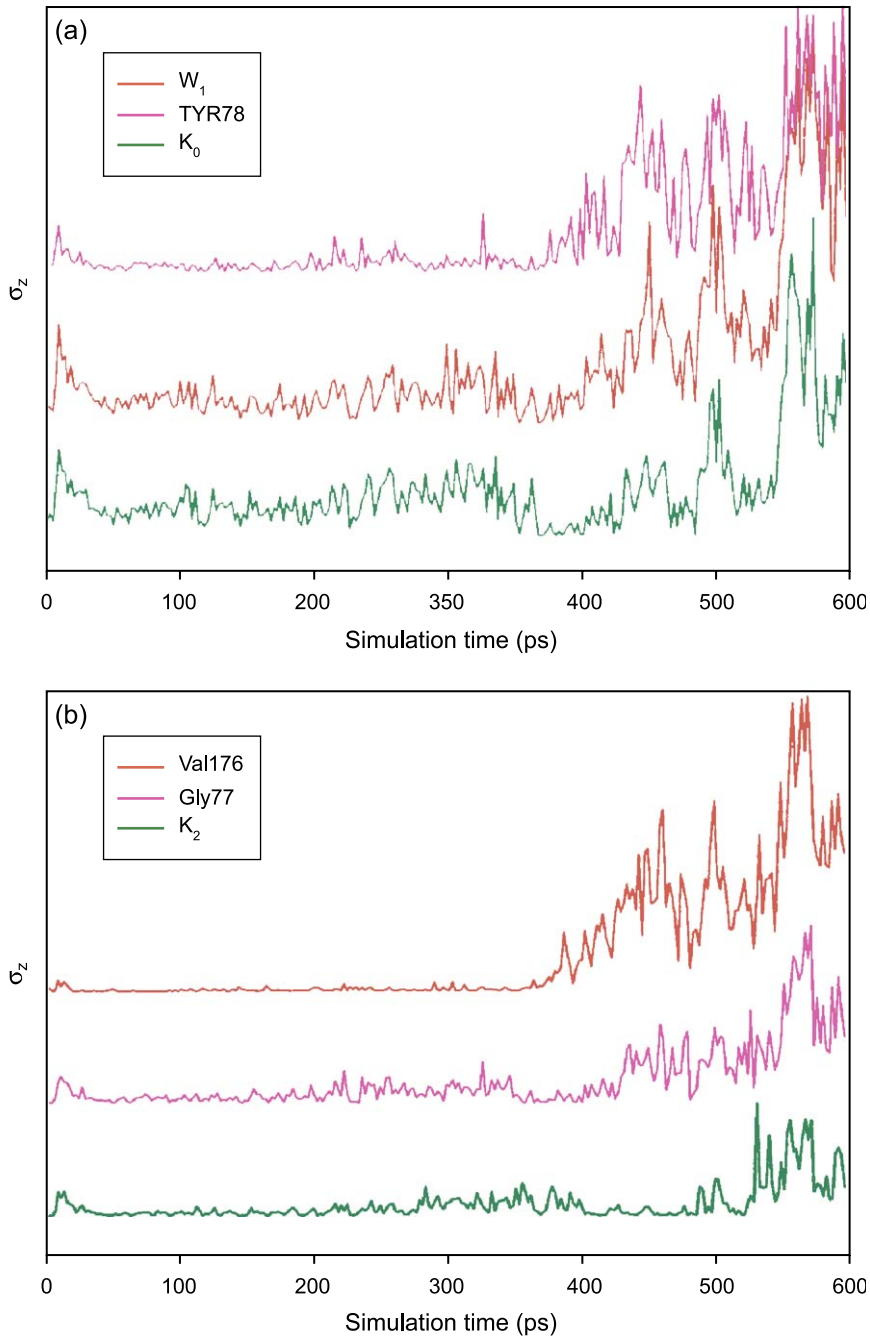

Fig. 9. (a)Square displacements σ_z of K_0 (green), W_1 (red) and Tyr78 residue (pink). (b) Square displacements σ_z of K_2 (green), Val76 (red) and Gly77 residue (pink).

We have shown that K_0 is found to be located deeper inside the filter because it tries to bind strongly with the oxygen atoms of Tyr78 carbonyl groups in order to optimize its electrostatic interactions. We retrieve a result already mentioned by Guidoni and Carloni [8] concerning the permeation of this ion. Indeed, K_0 needs to dehydrate in order to penetrate inside the filter at the extracellular mouth. Fig. 10 shows that the initial coordination number of oxygen is six while it reaches seven on average when K_0 is located deeper inside the filter. The search for the larger hydration shell could explained such a trend for K_0.

Finally, K_{cav} feels a regular increase of its number of oxygen coordination with the distance that corresponds to its encapsulation in the water pocket formed by the cavity. The first plateau at about 3 Å corresponds to eight oxygen neighbors, i.e. a complete first hydration shell.

To summarize this subSection, the results show that, except for K_2 ion which always keeps its maximum coordination with oxygen atoms (of the wall or of the

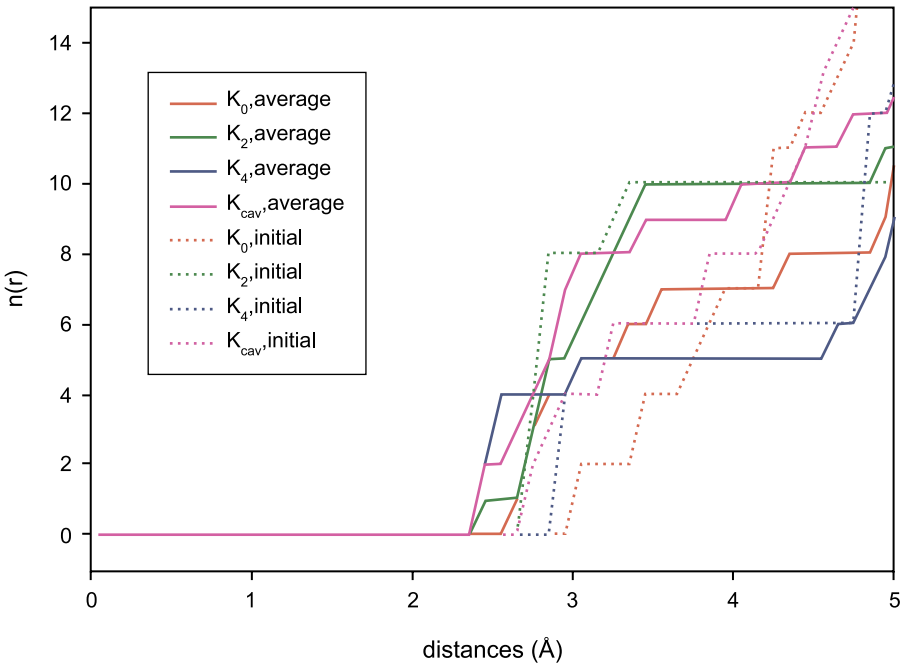

Fig. 10. Number of oxygen coordination as a function of distance for all the K^+ ions. Dotted lines correspond to initial starting configuration while full lines correspond to the average configuration obtained from MD.

two adjacent water molecules), there is a dominant trend for the other K^+ ions to optimize their coordination number.

5. Discussion

We have shown that motions of ions and water molecules inside the filter are concerted and sometimes strongly coupled to the motions of protein atoms belonging to the internal wall of the filter, depending on the site location. The autocorrelation functions for the four ions in the filter and the cavity (not shown here) take half their initial value after at least 300 ps, with a quasi-similar behavior. We can therefore consider that the dampings of all the ions are nearly the same. Moreover, a specific movement is observed when K_4 moves toward its metastable site. In that case, the central ion K_2 does not move a lot, while the two couples (K_0-W_1) and (K_4-W_3) move toward the intracellular sides. Indeed, even if we have seen that the electrostatic interactions of K_4 with carbonyl groups of Thr75 and hydration properties can explain the ascent of K_4 in the filter, it could be surprising that the second couple (K_0-W_1) moves also toward the center of the filter. If we expect diffusion of ions at the extracellular side (the intracellular side being closed by the gate), the two couples should logically move in the same direction. Another interesting feature is that diffusion effectively occurs if we let the system run more than 1 ns. This work has been already done by Bernèche and Roux [22] on the 3.2-Å resolution structure using the same equilibration protocol. In the 3.2-Å structure resolution, the sites were very stable and ions stayed in their sites during the equilibration. One might think that the structure itself can explain such differences. The main difference between the two structures corresponds to the 24 amino acids located at the end of side chains and in the water zone close to the membrane. The hypothesis that these 24 amino acids alter the K_4 and W_3 behavior and influence their displacements is improbable. Note that we have also verified that the filter throws out the ions after a larger time scale on the (NPT) ensemble. In this discussion part, we want to understand the dynamics of the ions which adopt a kind of breathing mode for motions and switch to diffusion on a larger time scale. Another question also arises: What is the origin of such peculiar motions? In fact, we have already underlined that these motions are induced by switching our molecular dynamics conditions from (NVT) to (NPT). But, what has happened physically? In this discussion part, we show that this is not a numerical artifact but more of a perturbation which could occur at any time and induce afterward the diffusion of ions.

To explain these peculiar behaviors on the displacements, we have built a simple mechanical model schematized on Fig. 11. It is composed of three superatoms moving along an axis. The displacements z_j of the jth atom with respect to its equilibrium position is assumed to be harmonic. We denote by k_1 and k_3 the spring force constants between the central atom (number 2) of mass m and the first and third atoms of mass M, respectively. This system has been modeled on the basis of our results in the

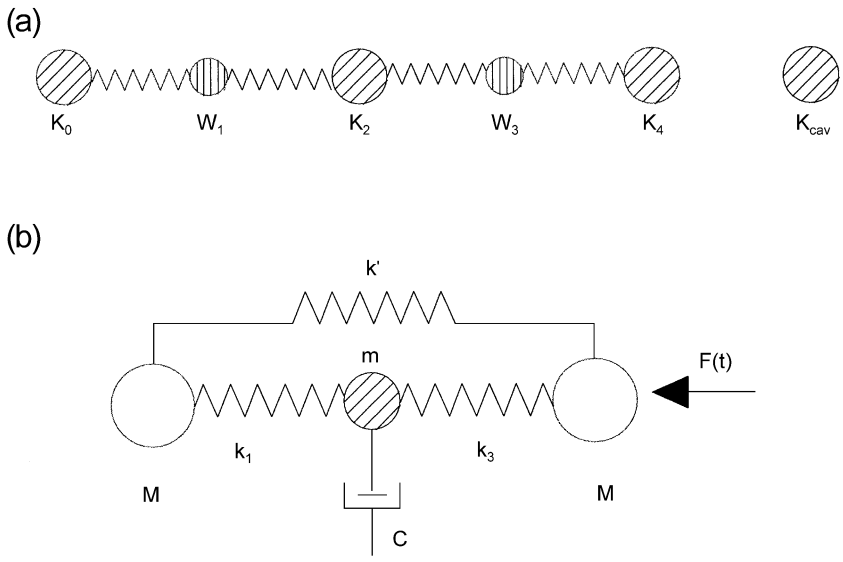

Fig. 11. Schematic representation of the mechanical model for the file.

above Section. In fact, we have seen that K^+ ions and water molecules contained in the two couples (K_0–W_1) and (W_3–K_4) move together and can thus be described in a first approximation each as a single superatom of mass $M = m_K + m_{H_2O}$. The central ion in this model schematises K_2, with a mass m_K. This ion has a singular behavior since we have seen before that K_2 is strongly coupled to the protein dynamics. Hence, we have introduced a damping constant c at that position only. It can be questioning how we can model the interactions within the KWKWK...K file by springs. Indeed, the electrostatic interactions are long-range and not harmonic but if we consider that the ions vibrate around their equilibrium positions without diffusing, this assumption appears licit over times shorter than those required for the ion diffusion. The additional k' force constant between the first and third atoms takes into account the non-local behavior of interactions. Finally, we assume that the system is forced on one side by an external force. This later takes the form $f(t) = F\cos(\omega\ t)$ with zero average value. This force can be due for instance to thermal fluctuations of K_{cav} in the cavity. Any other force responsible for the diffusion of the ions in the pore is disregarded here (no force due to ionic external/internal concentration gradient and to electropotential difference). It is applied on K_4 since we have shown that the correlation between K_4 and K_{cav} was good and K_{cav} plays a particular role, being surrounded by water molecules in the cavity (see Fig. 8). This important role has also been highlighted by Bernèche and Roux [16]. The dynamical equations of this system are thus written as:

$$\begin{aligned} M\frac{\partial^2 z_1}{\partial t^2} + (k_1 + k'\ )z_1 - k_1 z_2 - k'\ z_3 &= 0 \\ m\frac{\partial^2 z_2}{\partial t^2} + c\frac{\partial z_2}{\partial t} - k_1 z_1 + (k_1 + k_3)z_2 - k_3 z_3 &= 0 \\ M\frac{\partial^2 z_3}{\partial t^2} - k'\ z_1 - k_3 z_2 + (k_3 + k'\ )z_3 &= F\cos(\omega t) \end{aligned} \tag{3}$$

The spring constants k', k_1 and k_3 are not known, and we have thus introduced relative force constants with respect to k_1: $\alpha = k_1/k_3$, $b = k'/k_1$ as parameters so that $k'/k_3 = \alpha b$. We have also defined the relative mass $a = m/M$ (a is close to 0.7 in our case), the square eigenfrequencies $\omega_1^2 = k_1/M$ and $\omega_3^2 = k_3/M$ and the relative damping coefficient $\eta = c/(2m\omega_1)$. It should be noted that these parameters could be in principle be calculated. This could be very useful especially to appreciate if the motions of the KWKWK...K file are overdamped or underdamped. A similar work was performed by Straub et al. [35] for a simple isomerizing molecule embedded in a Lennard–Jones fluid. In particular, they show that the calculation of the velocity correlation functions could lead to the determination of a rough value of the friction coefficient. This determination is indeed feasible but not tractable in a straightforward way. This will be the object of a future modelling of the KcsA in its opened and closed states. Here, we have chosen to keep the damping and force constants as parameters.

The solutions z_j of the jth atom have the general form: $z_j(t) = Z_j(\omega)\cos(\omega\ t + \phi_j)$. Straightforward calculations show that the amplitudes $Z_j(\omega)$ solutions of Eq. (3) can be written as:

$$Z_1 = \frac{Z_{3s}}{D}\left[(1 + b(1 + \alpha - a\alpha\beta^2))^2 + 4\alpha^2\beta^2\eta^2\right]^{\frac{1}{2}}$$

$$Z_2 = \frac{Z_{3s}}{D}\left[1 + b(1 + \alpha) - \beta^2\right]$$

$$\begin{aligned} Z_3 = \frac{Z_{3s}}{D}\big[&(1 - a\alpha\beta^2 + (b - \beta^2)(1 + \alpha - a\alpha\beta^2))^2 \\ &+ 4\alpha^2\beta^2\eta^2(1 + b - \beta^2)^2\big]^{\frac{1}{2}} \end{aligned} \tag{4}$$

where the amplitudes are expressed in terms of the relative frequency $\beta = \omega/\omega_1$, and:

$$Z_{3s} = \frac{F}{k_3}$$

$$D^2 = \{(1+b-\beta^2)[(1+\alpha-a\alpha\beta^2)(1+\alpha b-\alpha\beta^2)-1] + \alpha^2(\beta^2-b)-\alpha(1+b)^2-\alpha^2b^2(1-a\beta^2)\}^2 + 4\alpha^2\beta^2\eta^2\{(1+b-\beta^2)(1+\alpha b-\alpha\beta^2)-\alpha b^2\}^2 \quad (5)$$

Fig. 12 shows typical behaviors of the dynamical amplification factors $\mu_j = Z_j/Z_{3s}$ ($j = 1-3$) as a function of β for $a = 0.7$, $\alpha = 1.0$ and $b = 0.1$. These parameters correspond to the same coupling constants of sites 1–2 and 2–3 while the coupling of 1–3 appears to be smaller by a factor 10. η is chosen to be equal to 1 in the present case which corresponds to critical damping. For the model depicted in Fig. 11, we retrieve the main characteristics already present in the molecular dynamics results. The central atom (namely K_2 ion) exhibits smaller amplitude than the two other atoms for typical ranges of β values. This behavior is still reinforced when the damping coefficient η increases. It should be noted that the number and position of resonances at peculiar β values depend on the choice of the parameter values. Nevertheless, as shown here, one resonance always occurs for β close to unity (in our case $\beta = 1.1$). Physically, this means that, when the oscillating external force due to the K_{cav} fluctuations in the cavity reaches the eigenfrequency ω_1, the two couples (K_0-W_1 and W_3-K_4) exhibit motions with very large amplitudes, leading eventually to the breaking of the KWKWK...K file. Examination of the phase coefficients ϕ_j with respect to β (not shown here) is also instructive since it is responsible for the atom motions after the damage of the KWKWKK file ($F = 0, \alpha = 0$ and $b = 0$). Two possible situations can be inferred with respect to the relative motions of the atoms at the moment when the file breaks. The first situation obtained for $\phi_3 - \phi_1 = \pi$ (phase opposition) corresponds to the draining of the channel while the second situation for $\phi_3 - \phi_1 = 0$ (in phase motions) could lead to the diffusion of the species inside the channel. The analysis of the in phase difference $\phi_3 - \phi_1$ should in principle clarify this situation, but unfortunately, this difference strongly depends on the values of the unknown damping constant η. We can nevertheless gain qualitative ideas from the present model. Near the resonance for $\beta \simeq 1.1$, the superatoms with mass M (at the extremities of the file) vibrate in quadrature ($\phi_3 - \phi_1 = 80°$) while in phase situation corresponding to diffusion would occur for larger values of $\beta \simeq 1.5$ and the phase opposition occurs for $\beta = 1$. Although this model cannot take into account the diffusion inside the pore because the only considered force is a fluctuating one with zero average, it is able to initiate large motions of the K^+ and water species in the filter sufficient to favor the jump from one site to an adjacent one.

6. Conclusion

To conclude this work, we have shown that the KcsA protein determined at 2-Å resolution is very stable in the presence of six sites occupied with the KWKWK...K

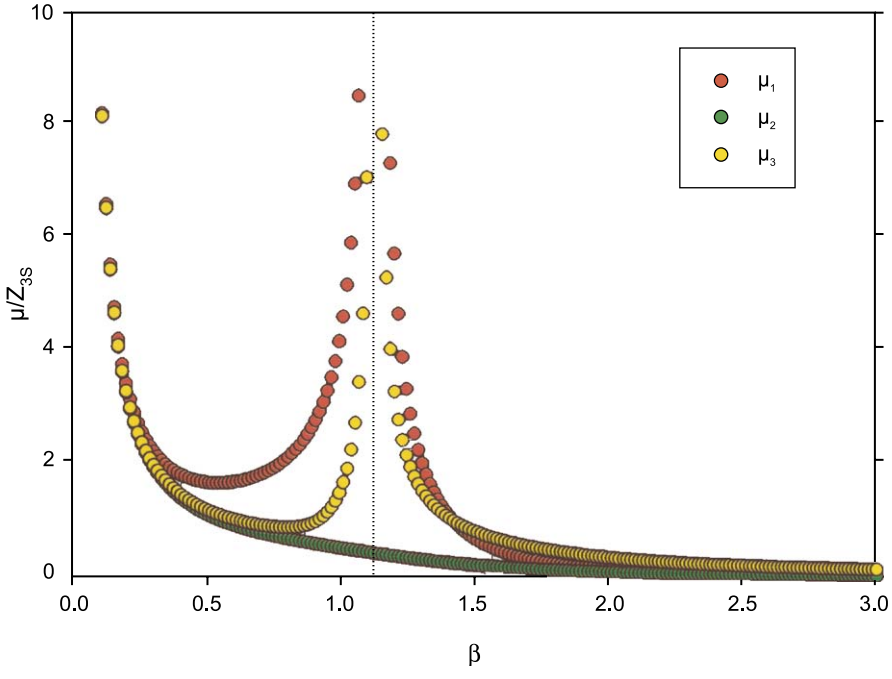

Fig. 12. Dynamical amplification factors associated to the groups 1, 2 and 3 (see Fig. 11) as a function of the relative frequency β.

sequence. The analysis of the dynamics within this file shows strong evidence for strongly correlated motions between the K^+ ions inside the filter and their adjacent water molecule, and between all the ions which participate in the file. The Molecular Dynamics simulations results can be, at least partially, interpreted on the basis of a simple dynamical model which exhibits resonances leading to the occurrence of large amplitude motions. We suggest that resonances within the file could favor the diffusion mechanism observed in this channel.

Acknowledgements

One of the authors (M.C) would like to thank P. Carloni for his kind hospitality during summer 2002. Pietro Vidossic is greatly acknowledged for his help to construct the KcsA model structure. Michele Cascella, Katrin Spiegel and Alejandro Giorgetti are also acknowledged for their implications in this work.

References

[1] H. Schrempf, O. Schmidt, R. Kummerlen, S. Hinnah, D. Muller, M. Betzler, T. Steinkamp, R. Wagner, A prokaryotic potassium ion channel with two predicted transmembrane segments from *Streptomyces lividans*, EMBO J. 14 (1995) 5170–5178.

[2] D.A. Doyle, J.M. Cabral, A. Pfuetzner, A. Kuo, J.M. Gulbis, S.L. Cohen, B.T. Chait, R. MacKinnon, The structure of the potassium channel: molecular basis of K^+ conduction and selectivity, Science 280 (1998) 69–77.

[3] J.H. Morais-Cabral, Y. Zhou, R. MacKinnon, Energetic optimization of ion conduction rate by the K^+ selectivity filter, Nature 414 (2001) 37–42.

[4] Y. Zhou, J.H. Morais-Cabral, A. Kaufman, R. MacKinnon, Chemistry of ion coordination and hydration revealed by a K^+ channel-Fab complex at 2.0 Å resolution, Nature 414 (2001) 43–48.

[5] B. Roux, S. Bernèche, W. Im, Ion channels, permeation, and electrostatics: insight into the function of KcsA, Biochemistry 39 (2000) 13295–13306.

[6] I.H. Shrivastava, M.P. Sansom, Simulations of ion permeation through a potassium channel: molecular dynamics of KcsA in a phospholipid bilayer, Biophys. J. 78 (2000) 557–570.

[7] T.W. Allen, A. Bliznyuk, A.P. Rendell, S. Kuyucak, S.H. Chung, The potassium channel: structure, selectivity and diffusion, J. Chem. Phys. 112 (2000) 8191–8204.

[8] L. Guidoni, P. Carloni, Potassium permeation through the KcsA channel: a density functional study, Biochim. Biophys. Acta 1563 (2002) 1–6.

[9] M.S.P. Sansom, I.H. Shrivastava, J.N. Bright, J. Tate, C. Capener, P. Biggin, Potassium channels: structures, models, simulations, Biochim. Biophys. Acta 1565 (2002) 294–307.

[10] L. Guidoni, V. Torre, P. Carloni, Potassium and sodium binding to the outer mouth of the K^+ channel, Biochemistry 38 (1999) 8599–8604.

[11] T.W. Allen, S. Kuyucak, S. Chung, Molecular dynamics study of the KcsA potassium channel, Biophys. J. 77 (1999) 2502–2516.

[12] T.W. Allen, S. Kuyucak, S. Chung, Molecular dynamics estimates of ion diffusion in model hydrophobic and KcsA potassium channels, Biophys. Chemist. 86 (2000) 1–14.

[13] P.C. Biggin, G.R. Smith, I.H. Shrivastava, S. Choe, M.P. Sansom, Potassium and sodium ions in a potassium channel studied by molecular dynamics simulations, Biochim. Biophys. Acta 1510 (2001) 1–9.

[14] V. Luzhkov, J. Åqvist, K^+/Na^+ selectivity of the KcsA potassium channel from microscopic free energy perturbation calculations, Biochim. Biophys. Acta 1548 (2001) 194–202.

[15] I.H. Shrivastava, D.P. Tieleman, P.C. Biggin, M.P. Sansom, K^+ versus Na^+ ions in a K channel selectivity filter: a simulation study, Biophys. J. 83 (2002) 633–645.

[16] S. Bernèche, B. Roux, Energetics of ion conduction through the K^+ channel, Nature 414 (2001) 73–77.

[17] P.C. Biggin, M.P. Sansom, Open-state models of a potassium channel, Biophys. J. 83 (2002) 1867–1876.

[18] I.H. Shrivastava, M.P. Sansom, Molecular dynamics simulations and KcsA channel gating, Eur. Biophys. J. 31 (2002) 207–216.

[19] T.W. Allen, S. Chung, Brownian dynamics study of an open-state KcsA potassium channel, Biochim. Biophys. Acta 1515 (2001) 83–91.

[20] S.H. Chung, S. Kuyucak, Ion channels: recent progress and prospects, Eur. Biophys. J. 31 (2002) 283–293.

[21] L. Guidoni, V. Torre, P. Carloni, Water and potassium dynamics inside the KcsA K^+ channel, FEBS Lett. 477 (2000) 37–42.

[22] S. Bernèche, B. Roux, Molecular dynamics of the KcsA K^+ channel in a bilayer membrane, Biophys. J. 78 (2000) 2900–2917.

[23] C. Capener, M.P. Sansom, Molecular dynamics simulations of a K channel model: sensitivity to changes in ions, waters, and membrane environment, J. Phys. Chem. 106 (2002) 4543–4551.

[24] V. Luzhkov, J. Åqvist, A computational study of ion binding and protonation states in the KcsA potassium channel, Biochim. Biophys. Acta 1481 (2000) 360–370.

[25] E. Perozo, New structural perspectives on K^+ channel gating, Structure 10 (2002) 1027–1029.

[26] Y. Jiang, A. Lee, J. Chen, M. Cadene, B.T. Chait, R. MacKinnon, Crystal structure and mechanism of a calcium-gated potassium channel, Nature 417 (2002) 515–521.

[27] D. Meuser, H. Splitt, R. Wagner, H. Schrempf, Exploring the open pore of the potassium channel from *Streptomyces lividans*, FEBS Lett. 462 (1999) 447–452.

[28] Y. Shen, Y. Kong, J. Ma, Intrinsic flexibility and gating mechanism of the potassium channel KcsA, Proc. Natl. Acad. Sci. U. S. A. 99 (2002) 1949–1953.

[29] M.L. Connolly, Solvent-accessible surfaces of proteins and nucleic acids, Science 221 (1983) 709–713.

[30] C. Miller, See potassium run, Nature 414 (1991) 23–24.

[31] U. Essmann, L. Perera, M.L. Berkowitz, T. Darden, H. Lee, L.G. Pedersen, A smooth particle mesh Ewald method, J. Chem. Phys. 103 (1995) 8577–8593.

[32] W.L. Jorgensen, J. Chandrasekhar, J.D. Madura, Comparison of simple potential functions for simulating liquid water, J. Chem. Phys. 79 (1983) 926–935.

[33] H.J.C. Berendsen, J.P.M. Postma, W.F. Van Gunsteren, A. Di Nola, J.R. Haak, Molecular dynamics with coupling to an external bath, J. Chem. Phys. 81 (1984) 3684–3690.

[34] A.L. Hodgkin, R.D. Keynes, The potassium permeability of a giant nerve fibre, J. Physiol. 128 (1955) 61–88.

[35] J.E. Straub, M. Borkovec, B.J. Berne, Molecular dynamics study of an isomerizing diatomic in a Lennard–Jones fluid, J. Chem. Phys. 89 (1988) 4833–4847.